

# Is the Shanxi rift of northern China extending?

Jiankun He

Institute of Geology and Geophysics, Chinese Academy of Sciences, Beijing, China

Mian Liu

Department of Geological Sciences, University of Missouri-Columbia, Missouri, USA

Yanxing Li

First Crustal Deformation Monitoring Center, China Seismological Bureau, Tianjin, China

Received 3 October 2003; revised 29 October 2003; accepted 4 November 2003; published 10 December 2003.

[1] The Shanxi rift in northern China is marked by intensive seismicity, including many devastating historic earthquakes. Geological and seismological evidence show 0.5–1.6 mm/yr extension across the rift, and previous GPS results indicated an extension rate of  $4 \pm 2$  mm/yr. We show here newly compiled GPS data that indicate coherent crustal motion and no clear sign of extension across the rift. We reconcile the discrepancy between geological observations and GPS results in a simple viscoelastic finite element model with timescale-dependent crustal deformation. The GPS velocities can be fit by a model with a near elastic upper crust, consistent with predominantly interseismic deformation. The geological rate of extension is predicted when viscous creep of the crust is dominant, driven by the gravitational potential energy arising from the heterogeneity of crustal structure. **INDEX TERMS:** 1208 Geodesy and Gravity: Crustal movements—intraplate (8110); 8107 Tectonophysics: Continental neotectonics; 8109 Tectonophysics: Continental tectonics—extensional (0905); 8122 Tectonophysics: Dynamics, gravity and tectonics; 8159 Tectonophysics: Rheology—crust and lithosphere. **Citation:** He, J., M. Liu, and Y. Li, Is the Shanxi rift of northern China extending?, *Geophys. Res. Lett.*, 30(23), 2213, doi:10.1029/2003GL018764, 2003.

## 1. Introduction

[2] The Shanxi rift in northern China is an intracontinental rift zone with many devastating earthquakes, including the 23 January 1556 Huaxian earthquake ( $M \geq 8$ ), the most deadly earthquake in human history that killed  $\sim 830,000$  people [Ming *et al.*, 1995]. Chinese historic records show at least 32 earthquakes with magnitude  $\geq 6$  occurred within the rift since 231 AD (Figure 1) [Ming *et al.*, 1995]. Modern seismicity indicates active rifting (Figure 1). Wesnousky *et al.* [1984] estimated a coseismic extension rate around  $\sim 1.0$  mm/yr based on seismic moment data. This is close to the 0.5–1.6 mm/yr extension rate averaged over the Late Pliocene-Quaternary time [Zhang *et al.*, 1998].

[3] Given the potential of earthquake hazard in the Shanxi rift and adjacent regions, several Chinese agencies have conducted a series of Global Positioning System (GPS) field campaigns since 1992. The earlier results indicated  $\sim 4 \pm 2$  mm/yr active extension across the Shanxi rift [Shen *et al.*, 2000]. However, the velocity jump across

the Shanxi rift became obscure when more GPS data were compiled [Wang *et al.*, 2001a].

[4] Is the Shanxi rift extending? We address this question by first presenting the newly compiled GPS results. We then reconcile the apparently discrepant GPS, seismological, and geological data using a simple geodynamic model that simulates crustal deformation at different timescales.

## 2. Geological Background and GPS Results

[5] The Shanxi rift, bordered by the Ordos Massif to the west and the Taihang Shan Uplift to the east, is located within the North China Block, which is part of the Sino-Korean Achaean shield that became reactivated since late Mesozoic [Griffin *et al.*, 1998] (Figure 1). Extension of the Shanxi rift may have started in Miocene [Zhang *et al.*, 1998], but the present graben formed mainly since Pliocene [SSBRG, 1988; Xu *et al.*, 1993].

[6] The GPS data collected by the China Seismological Bureau during 1992–1996 indicated  $4 \pm 2$  mm/yr extension across the Shanxi rift [Shen *et al.*, 2000]. An expanded data set, however, showed more scattering of the GPS site velocities; the signals of active extension vanished [Wang *et al.*, 2001a]. To resolve the discrepancies between these datasets, we have compiled the latest GPS data with 447 site velocities measured in 1999 and 2001 by the First Crustal Deformation Monitoring Center (FCDMC) of China Seismological Bureau. The measurements were made with Ashtech Z-12 receivers. The data processing was the same as reported by Shen *et al.* [2000]. We used the GAMIT software to obtain loosely constrained daily solutions for the station positions and satellite orbits. The data were then combined with 16 global IGS solutions produced by the Scripps Orbital and Position Analysis Center (SOPAC) using the GLOCK software to get the commonly shared parameters. The final station positions and site velocities were derived using the QOCA software in the ITRF2000 reference frame.

[7] The new data are plotted together with previously published datasets under the same confidence level. Because the data of Wang *et al.* [2001a] were processed differently from Shen *et al.* [2000] and this study, we only compare with the dataset from Shen *et al.* [2000]. Figure 2a shows no clear sign of active extension across the Shanxi rift, consistent with the results of Wang *et al.* [2001a]. In Figure 2b, we plotted the new GPS data onto the same profile used in Shen *et al.* [2000]. It shows that the velocity jump across

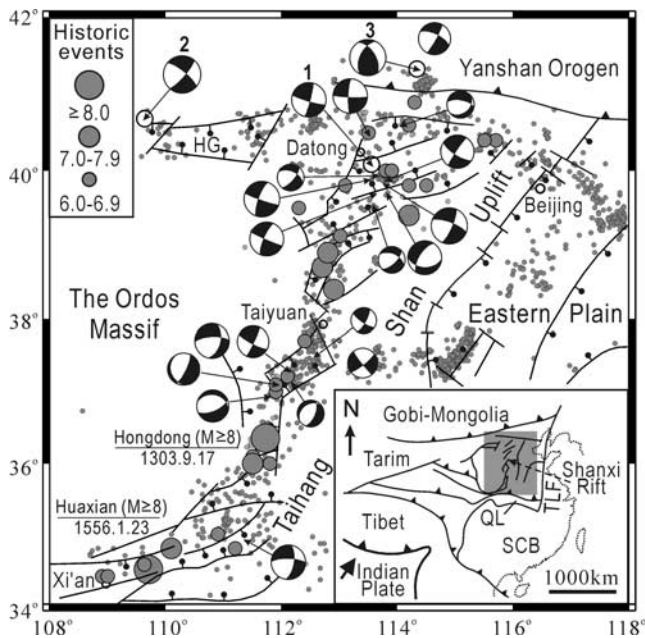


**Figure 1.** Major faults and seismicity in the Shanxi rift and surrounding region. The inset shows the plate tectonic setting. Thrust and normal faults are represented by the teeth line and ball-head line, respectively. The shaded circles are historic earthquakes ( $M \geq 6.0$ ). Small dots are earthquakes ( $M \geq 3$ ) from 1973–2003. Focal mechanism solutions are for selected modern earthquakes ( $M \geq 4$ ) [http://www.seismology.harvard.edu; Zhang *et al.*, 1990]. Events 1, 2, and 3 are the 1991/03/26  $M = 6.1$  Datong, 1996/05/03  $M = 6.6$  Baotou and 1998/01/10  $M = 6.2$  Zhangbei earthquakes, respectively. SCB, South China Block; QL, the Qinling orogen; TLF, the Tan-Lu fault; HG, the Hetao graben.

the Shanxi rift reported in Shen *et al.* [2000] vanished in the expanded dataset.

### 3. Reconcile the Discrepant Observations

[8] The 1991 Datong earthquake ( $M \sim 6.1$ ) located in the northern part of the Shanxi rift (Figure 1), an area covered during the 1992–1996 GPS measurements [Shen *et al.*, 2000], may have affected the velocity of some of the sites near the epicenter, but the post-seismic creep was unlikely to affect most of the GPS stations covering the entire North China Block. Although intrinsic errors of the present GPS data could have contributed to the discrepancy between the different datasets, the lack of clear signs of active extension across the entire length of the Shanxi rift may be better explained by the timescale-dependent crustal deformation [Liu *et al.*, 2000a].

[9] Since the 1991 Datong earthquake, there have been only two moderate events ( $M \sim 6$ ) near the northern edge of the North China Block and no large earthquakes within the Shanxi rift, thus the GPS data reflect largely interseismic deformation across the Shanxi rift when most of the faults remain locked. We developed a simple geodynamic model to simulate crustal deformation at two timescales: the short-term interseismic deformation represented by the GPS data, and the long-term deformation reflected in the geological

observations and to some extent in the accumulated earthquake data. The model is two-dimensional (Figure 3a), based on the TECTON finite element codes [Melosh and Raefsky, 1981] and assumes a viscoelastic rheology. The top of the model is a free surface with simplified topography. The Winkler springs are used on density boundaries (the reference surface, defined at the Eastern Plain, and the base of the crust) to simulate restoring forces [Williams and Richardson, 1991]. The present GPS data indicates a weak ESE compression over the entire North China Block (see Figure 2 and Wang *et al.* [2001a]). We use 8.7 mm/yr in the Ordos massif and 7.0 mm/yr in the Eastern Plain, all with respect to stable Eurasia, as the velocity boundary condition.

[10] If aseismic creep is negligible, the simplest way to simulate the interseismic crustal deformation with all active faults locked is to assume an elastic upper crust. The resulting surface velocity field is close to a linear interpo-

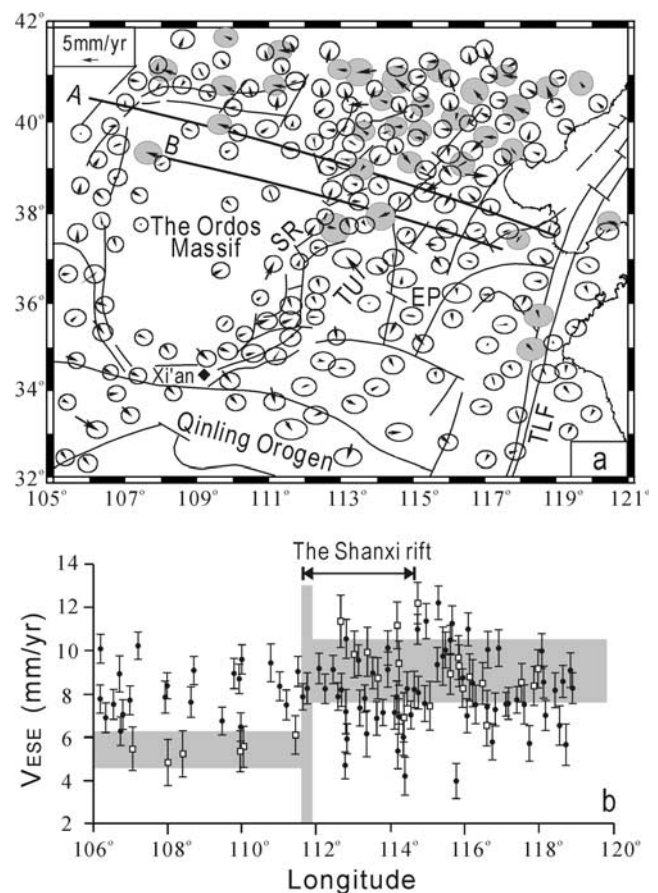


**Figure 2.** (a) GPS residual velocities around the Shanxi rift with respect to the Xi'an permanent GPS station within the NUVEL-1A reference frame. Error ellipses represent 95% confidence level. The velocities with shaded error ellipses are from 1992 to 1996 [Shen *et al.*, 2000]. Only selected sites were shown for clarity. Line A is the velocity profile in (b). Line B is the transect bases on which the numerical model shown in Figure 3a was built. (b) GPS site velocities relative to stable Eurasia, plotted along an ESE profile (location in (a)) within a 150 km wide swath. The square symbols are velocities from Shen *et al.* [2000] showing extension across the Shanxi rift. SR, the Shanxi rift; TU, the Taihang Shan Uplift; EP, the Eastern Plain.

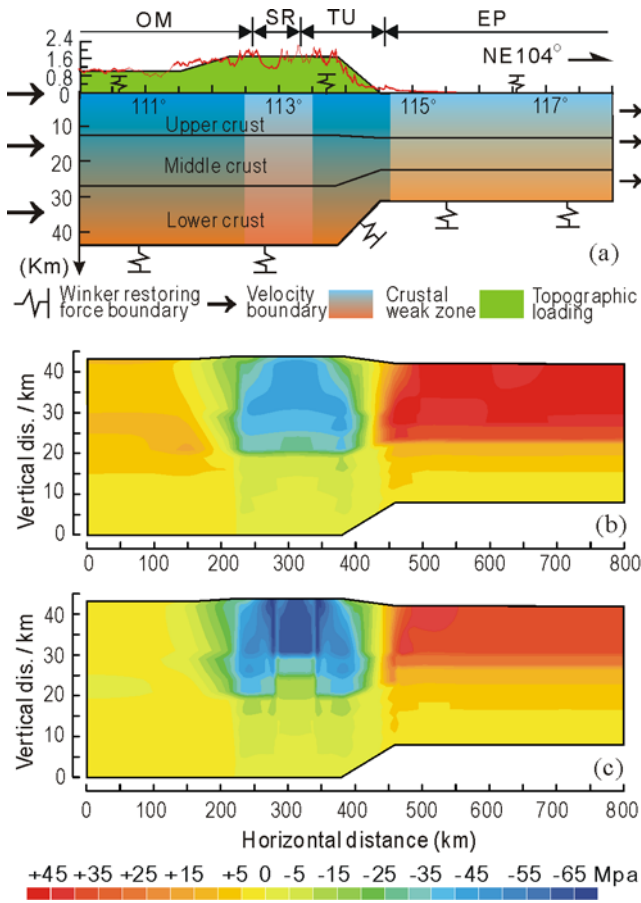


**Figure 3.** (a) Geometry and boundary conditions of the finite element model. The model surface is simplified from GTOPO-30 database, and the bottom approximates the Moho discontinuity [Ma, 1989; Xu *et al.*, 1993]. See text for details. (b) Predicted differential stress ( $\sigma_{xx} - \sigma_{zz}$ ) for a model with laterally homogeneous rheology. The cold color shows negative values ( $\sigma_{xx} < \sigma_{zz}$ ), indicating extension; the warm colors indicate compression. (c) Predicted differential stress with a weaker rheology in the Shanxi rift and the Eastern Plain. Abbreviations are explained in Figure 2.

lation of the applied boundary velocities, which fits the GPS velocities reasonably well (Figure 2). Similar results can be obtained by assuming a high ( $>10^{25}$  Pa s) effective viscosity for the upper crust [Liu *et al.*, 2000a].

[11] To simulate long-term stress state and crustal deformation, we assumed a viscoelastic upper crust and a power-law fluid middle-lower crust with temperature and strain rate dependent viscosity [Williams and Richardson, 1991]. The values of rheological parameters for the Maryland diabase and the Westly granite [Kirby and Kronenberg, 1987] were used to approximate the lower and middle crust, respectively. Figure 3b shows the predicted non-lithostatic differential stresses ( $\sigma_{xx} - \sigma_{zz}$ ) for a case with laterally homogeneous rheology. The results here are calculated over a timescale of a few million years, much greater than the viscous relaxation time (typically a few thousand years). In such cases the elastic effects become negligible, and the stress field is controlled by viscous creep [Liu *et al.*, 2000b]. The upper crustal viscosity is taken to be  $7 \times 10^{24}$  Pa s for long-term crustal deformation [England and Houseman,

1986], and temperature-dependent rheology of the middle-lower crust is determined by a linear temperature profile that changes from  $0^\circ\text{C}$  at the model surface to  $647^\circ\text{C}$  at the base of the crust, simplified from the average geotherm and heat flow data in the North China Block [Hu *et al.*, 2000]. The resulting effective viscosity is between  $10^{23}$  and  $10^{22}$  Pa s in the middle-lower crust. The model results indicate that most of the North China Block, especially the Eastern Plain, is under tectonic compression, consistent with the widespread Late Cenozoic compressive structures in Eastern Plain [Wang *et al.*, 2001b]. However, over the Shanxi rift and the western part of the Taihang Shan uplift, the stress state in the upper crust is predominantly extensional ( $\sigma_{zz} > \sigma_{xx}$ ) because of the topographic loading, or equivalently, the gravitational buoyancy force arising from the uplifted landmass [Liu *et al.*, 2000b; Molnar and Lyon-Caen, 1988]. The differential stresses are low in the middle-lower crust because of the relatively lower effective viscosity there.

[12] The real crustal rheology is certainly not uniform as assumed in Figure 3b. The surface heat flux within the Shanxi rift and many parts of the Eastern Plain is abnormally high [Hu *et al.*, 2000]. In Figure 3c, we reduced the upper crustal viscosity from  $7 \times 10^{24}$  to  $3 \times 10^{24}$  Pa s in the Shanxi rift and the Eastern Plain, and increased the temperature by 20–40°C in the middle-lower crust under these two regions, effectively reducing the middle-lower crust viscosity to  $10^{22}$  and  $10^{21}$  Pa s. Whereas the general pattern of the predicted differential stress remains the same (Figure 3c), the extensional stresses are higher and more concentrated within the Shanxi rift than in Figure 3b.

[13] Figure 4 shows the predicted surface velocity associated with the different cases of rheologic structures. The GPS data, which show a near linear trend of WNW-ESE

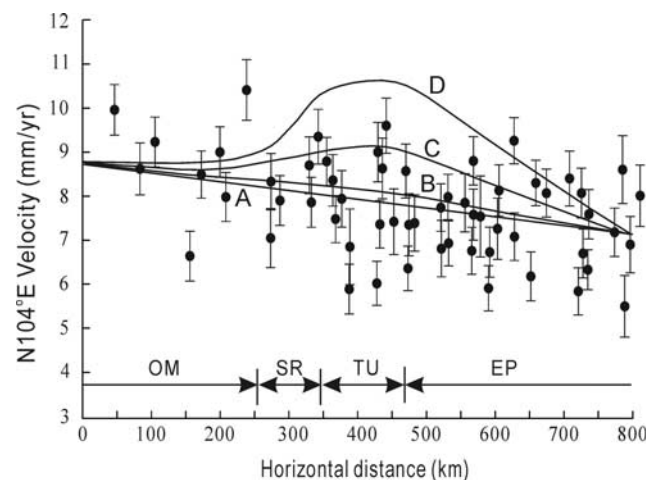


**Figure 4.** Comparison of the GPS data with the predicted surface velocities. GPS data are from a 150 km wide swath along the model profile shown in Figure 2. Curve A is a linear fit to the GPS data, curve B is predicted by assuming a stiff (viscosity =  $10^{27}$  Pa s) upper crust, curve C is from the model shown in Figure 3b, and curve D is from the model shown in Figure 3c. The positive velocity slope over the Shanxi rift (SR) and the Taihang Shan Uplift (TU) in curved C and D indicates extension.

compression (curve A), can be fit by the interseismic model in which all the active faults are locked in the stiff upper crust (effective viscosity  $\sim 10^{27}$  Pa s) underlying by a viscous middle-lower crust (effective viscosities  $10^{23} \sim 10^{22}$  Pa s) (curve B). At geological timescales, both the upper and lower crust deform as viscous media, and the predicted surface velocity shows extension in the Shanxi rift and compression in the Eastern Plain. The extension rate is  $< 0.3$  mm/yr (curve C) for a laterally homogeneous crust as shown in Figure 3b. With a weaker rheology assumed for the Shanxi rift and the Eastern Plain as described in Figure 3c, the extension rate increases to  $\sim 1.2$  mm/yr (curve D), similar to that derived from geological and seismological data [Wesnousky *et al.*, 1984; Zhang *et al.*, 1998]. Because the thermal-rheological structure is not well constrained, the exact values of the predicted extension rates need to be taken with caution.

#### 4. Discussion and Conclusions

[14] We have shown that the previously reported GPS velocity change that indicate active extension of the Shanxi rift become obscure when more recent data are compiled. Although further measurements will reduce the uncertainties of the GPS data, a more significant explanation for the GPS data may be the timescale-dependent crustal deformation [Liu *et al.*, 2000a]. Measured over a short period (typically a few years), GPS data often reflect mainly interseismic deformation when the active faults remain locked. This explains the smooth GPS velocities over the Shanxi rift and many other regions of known active crustal deformation, such as the Central Andes [Kendrick *et al.*, 2001; Leffler *et al.*, 1997] and the Himalayan-Tibetan plateau [Wang *et al.*, 2001a]. There may be transient strains near each individual fault associated with viscous relaxation in the ductile lower crust or aseismic creep on the faults, but dense and carefully designed GPS stations are needed to capture such subtle signals. On the other hand, seismological and geological data, representing crustal deformation over longer timescales, indicate that crustal extension in the Shanxi rift has been active. The cause of the Shanxi rift may be numerous and is debated [Yin, 2000]. Our results show that the gravitational potential energy arising from the heterogeneity of crustal thickness and thermal structure may be a major factor.

[15] GPS and other space-based geodetic measurements have been revolutionizing the studies of crustal deformation. However, given the timescale-dependence of rock rheology, it is important to understand how crust deforms at different timescales. The GPS data presented here cannot rule out active extension in the Shanxi rift. Given the history of devastating earthquakes in the Shanxi rift and the large population in the surrounding regions, continuous and carefully designed GPS measurements are needed to improve our understanding of the potential earthquake hazard.

[16] **Acknowledgments.** We are grateful to Min Wang, Jinhua Zhang, and the GPS team at the FCDMC for assistance in data collection and processing. The manuscript benefited from helpful reviews by Z.-K. Shen and an anonymous reviewer. This work was supported by Chinese Academy of Sciences (No50212910, KZCX1-07). Liu acknowledges

support by NSF grant EAR-0207200, the Research Board of the University of Missouri, and NSF of China grant 40228005.

#### References

- England, P. C., and G. A. Houseman, Finite strain calculations of continental deformation 2. Comparison with the India-Asia collision, *J. Geophys. Res.*, *91*, 3664–3676, 1986.
- Griffin, W. L., A. D. Zhang, S. Y. O'Reilly, and C. C. Ryan, Phanerozoic evolution of the lithosphere beneath the Sino-Korean craton, in *Mantle dynamics and plate interactions in east Asia*, edited by M. Flower, S. L. Chung, C. H. Lo, and T. Y. Lee, pp. 107–126, AGU, Geodynamics series 27, 1998.
- Hu, S.-B., L.-J. He, and J.-Y. Wang, Heat flow in the continental area of China: A new data set, *Earth Planet. Sci. Lett.*, *179*, 407–419, 2000.
- Kendrick, E., M. Bevis, R. J. Smalley, and B. Brooks, An integrated crustal velocity field for the central Andes, *Geochem. Geophys. Geosyst.*, *2*, doi:10.1029/2001GC000191, 2001.
- Kirby, S., II, and A. K. Kronenberg, Rheology of the lithosphere: Selected topics, *Rev. Geophys.*, *25*, 1219–1244, 1987.
- Leffler, L., S. Stein, A. Mao, T. Dixon, M. Ellis, L. Ocala, and I. S. Sacks, Constraints on the present-day shortening rate across the Central Eastern Andes from GPS measurements, *Geophys. Res. Lett.*, *24*, 1031–1034, 1997.
- Liu, M., Y. Yang, S. Stein, Y. Zhu, and J. Engeln, Crustal shortening in the Andes: Why do GPS rates differ from geological rates?, *Geophys. Res. Lett.*, *27*, 3005–3008, 2000a.
- Liu, M., Y. Shen, and Y. Yang, Gravitational collapse of orogenic crust: A preliminary 3D finite element study, *J. Geophys. Res.*, *105*, 3159–3173, 2000b.
- Ma, X.-Y., Lithospheric dynamics atlas of China (*in Chinese*), 68 pp., China Cartographic Publishing House, Beijing, 1989.
- Melosh, H. J., and A. Raefsky, A simple and efficient method for introducing faults into finite element computations, *Bull. Seismo. Soc. Am.*, *71*, 1391–1400, 1981.
- Ming, Z.-Q., G. Hu, Z. X. Jiang, S. C. Liu, and Y. L. Yang, Catalogue of Chinese Historic strong Earthquakes from 23 AD to 1911 (*in Chinese*), 514 pp., Seismological publishing House, Beijing, 1995.
- Molnar, P., and H. Lyon-Caen, Some simple physical aspects of the support, structure, and evolution of mountain belts, *Geol. Soc. Am. Spec. Paper*, *218*, 179–207, 1988.
- State Seismological Bureau Research Group (SSBRG), Active fault system around the Ordos, (*in Chinese*), 335 pp., Seismological Press, Beijing, 1988.
- Shen, Z.-K., C. Zhao, An Yin, Y. Li, and D. D. Jackson, Contemporary crustal deformation in east Asia constrained by Global Positioning System measurements, *J. Geophys. Res.*, *105*, 5721–5734, 2000.
- Wang, Q., P.-Z. Zhang, J. T. Freymueller, R. Bilham, K. M. Larson, X. Lai, X. You, Z. Niu, J. Wu, Y. Li, J. Liu, Z. Yang, and Q. Chen, Present-Day Crustal Deformation in China Constrained by Global Positioning System Measurements, *Science*, *294*, 574–577, 2001a.
- Wang, T. H., Z. C. Wang, Z. J. Zhao, X. Y. Cai, H. G. Wang, and Y. L. Chi, Inversion structure in China petroleum provinces (*in Chinese*), 563 pp., Petroleum Industry Press, Beijing, 2001b.
- Wesnousky, S. G., L. M. Jones, C. H. Scholz, and Q. Deng, Historical seismicity and rates of crustal deformation along the margins of the Ordos block, North China, *Bull. Seism. Soc. Am.*, *74*, 1767–1783, 1984.
- Williams, C. A., and R. M. Richardson, A rheological layered three-dimensional model of the San Andreas Fault in central and southern California, *J. Geophys. Res.*, *96*, 16,597–16,623, 1991.
- Xu, X.-W., X.-Y. Ma, and Q.-D. Deng, Neotectonic activity along the Shanxi rift system, China, *Tectonophysics*, *219*, 305–325, 1993.
- Yin, A., Mode of Cenozoic east-west extension in Tibet suggesting a common origin of rifts in Asia during the Indo-Asian collision, *J. Geophys. Res.*, *105*, 21,745–21,759, 2000.
- Zhang, C., X. L. Zhao, K. X. Qu, J. G. Xiu, and Z. X. Yao, China earthquake focal mechanisms (*in Chinese*), 466 pp., Academic Book Publishing House, Beijing, 1990.
- Zhang, Y. Q., J. L. Mercier, and P. Vergely, Extension in the graben systems around the Ordos [China], and its contribution to the extrusion tectonics of south China with respect to Gobi-Mongolia, *Tectonophysics*, *285*, 41–75, 1998.

J. He, Institute of Geology and Geophysics, Chinese Academy of Sciences, Beijing 100029, China. (jkhe@mail.igcas.ac.cn)

M. Liu, Department of Geological Sciences, University of Missouri-Columbia, MO 65211, USA.

Y. Li, First Crustal Deformation Monitoring Center, China Seismological Bureau, Tianjin 300180, China.